

AMORPHOUS COMPOSITE PHOTOCATALYSTS: A NEW GENERATION OF ACTIVE MATERIALS FOR ENVIRONMENT APPLICATION

Cristian. CHIS^a, Alexis EVSTRATOV^a, Anatoly MALYGIN^b, Anatoly MALKOV^b, Pierre GAUDON^a, Jean-Marie TAULEMEUSSE^a

a. Ales Hight School of Mining, 6 avenue de Clavieres Ales Cedex, France

b. State Institute of Technology , 26 Moskovsky pr., 190013, Saint-Petersburg, Russia

Abstract: Currently, only the semiconductors (usually in the form of nanometric particles) are considered to be efficient photocatalysts. The most wide-spread photocatalytic agent is Degussa P25. Unfortunately, this prefabricated crystalline species is not specially adapted for application because of the well-known handling problems. At present, any non-crystalline material is really recognized to be an active photocatalyst. This work attempts to highlight the photocatalytic properties of non-crystalline composite materials containing nanosized amorphous TiO₂ chemically fixed on different mineral supports. For comparative tests, a series of composite photocatalysts containing crystalline TiO₂ nano-aggregates was also fabricated. In both cases, the elaboration technique was based on the principles of the Chemical Vapor Deposition - Molecular Layering (CVD-ML) method. The non-crystalline TiO₂ nano-composites manifest both significant photocatalytic activities exceeding that of Degussa P25 (test reactions – trichloroethane and toluene oxidation in gaseous phase) and important sterilization capacities under UV-A and sunlight irradiation.

Keywords: photocatalysis; amorphous nanostructures; composite materials

1. INTRODUCTION

The photocatalytic phenomenon in crystalline semiconductor structures is based on their photonic excitation by near UV and visible light. The photo-excitation leads to the creation of “electron - positive hole” (e⁻, h⁺) pairs resulting from the passage of electrons from the semiconductor valence band to its conduction band through the forbidden zone. The free charge carriers reach the surface of the solid and attack oxygen and water molecules pre-adsorbed over the surface transforming them into active forms (O⁻, O²⁻, OH⁻). These species, in their turn, react with impurity adsorption complexes and degrade them, in a favourable case, into final oxidation products (Zhao et al. 2003) (fig. 1).

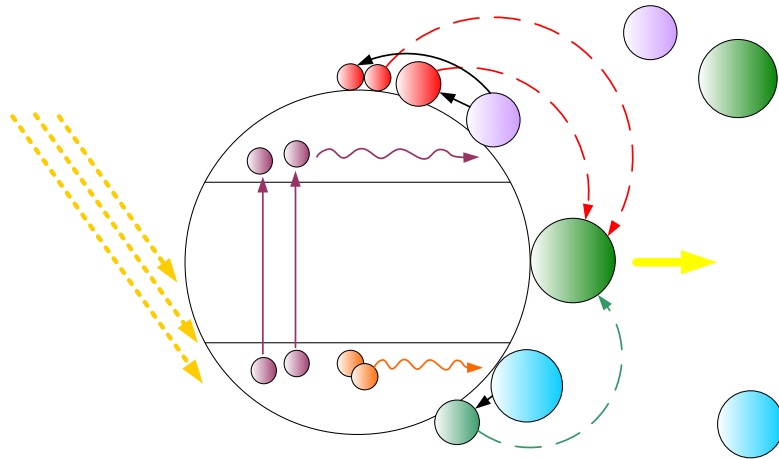


Fig. 1. Photocatalytic phenomenon in crystalline semiconductor structures

One of the commercially available active materials, Degussa P25 (crystalline TiO_2 nanoparticles containing 70% of anatase and 30% of rutile), has now become a reference product (Amine-Khodja et al. 2005). However, even if the particle sizes are highly appropriate to this requirement, the main disadvantage of all prefabricated powder forms is the well-known handling difficulties caused by the necessity to operate with powder species in their initial “free” state. Several modern techniques Plasma Assisted Metallo-Organic CVD (Lecheng et al. 1999), Laser Photo-Induced CVD (Wang et al. 2004), Arc Ion Plating (Chang et al. 2006), Dip-coating (Ma et al. 2001), Photo-Inducted Sol-Gel (Kaliwoh et al. 2000), Sputtering (Stamate 2000), etc.] have been recently developed in order to grow nanosized semiconductor crystals *in situ* using various template surfaces. The complexities these techniques and their expensiveness condemn them to remain, at least for the time being, at laboratory scale. On the other hand, besides some rare publications supposing an eventual photocatalytic activity of non-crystalline TiO_2 structures (e.g. Yumoto et al. 2002), no amorphous material is currently recognized as an active photocatalyst.

The main objective of this research was to evaluate the feasibility of non-crystalline composite systems containing TiO_2 amorphous aggregates chemically fixed on porous mineral supports as photocatalytic cleaning and sterilisation materials when exposed to UV-A (“black light”) and sunlight irradiation.

2. MATERIALS AND METHODS

2.1. Sample elaboration

The composite samples “amorphous or crystalline TiO_2 aggregates – mineral support” were elaborated using two fabrication techniques (CVD-MLM1 and CVD-MLM2, respectively), both based on Chemical Vapour Deposition - Molecular Layering method (Malygin 1999). Titanium tetrachloride TiCl_4 (ACROS Organics)

was chosen as TiO₂ precursor. Pure oxides - silica SiO₂ (ACROS Organics) and activated alumina γ -Al₂O₃ (Axens-IFP Group Technologies) were selected as mineral supports for the photocatalytic composites. Degussa P25 (ACROS Organics), was selected as reference product.

2.2. Experimental set-up

The operational parameters of the experimental set-up with a radial photocatalytic reactor are cited in Table 1. The toluene total oxidation was chosen as test reaction.

Table 1. Operational parameters of the experimental set-up

| Parameter | Value |
|--|---|
| Toluene vapour initial concentrations | $C_0 = 30 \div 35 \text{ mg/m}^3$ |
| Gas relative humidity | $\varphi = 0$ |
| Gas residence time in the reaction zone | $\Delta\tau \approx 12 \div 15 \text{ s}$ |
| Length and diameter of the test reactor (glass tube) | $L = 17 \text{ cm}, D = 4 \text{ cm}$ |
| Total mass of composite samples | $M_{\text{total}} = 1000 \pm 50 \text{ mg}$ |
| TiO ₂ content in samples | $M_{\text{cat}} = 30 - 60 \text{ mg}$ |
| Characteristics of the radiation source | « Black light » Philips lamp T L-6, $\lambda = 365 \text{ nm}, \text{ electric power} = 6\text{W}$ |

Gas chromatography was used to measure the toluene contents in the gas mixtures upstream and downstream from the photocatalytic reactor (Hewlett-Packard 890 Series II and Finningan Trace GC ULTRA gas chromatographs, (FID)).

2.3. Sterilisation capacity protocol

Genetically modified *Escherichia coli* (source – INRA, France) were selected as test bacteria. After the bacterial impregnation, the samples were exposed to sunlight and UV “black light” for 20 min. Afterwards the bacteria from all the samples were transferred to Petrie dishes containing nutritive gel and conserved in dark for 20 hours at 37°C in order to promote the development of bacterial colonies.

2.4. Sample characterization

The TiO₂ mass concentrations in the composite samples were determined by atomic emission spectroscopy (ICP JY 2000). The titanium dioxide phase was dissolved by treating the sample in solution (H₂SO₄) during 1 hour at 90°C under permanent agitation. The crystalline states were investigated by high performance XRD analysis (D8 Harque BRUKER X-ray Diffractometer, $\lambda \text{ K}\alpha \text{ Cu} = 1,5406\text{\AA}$). The morphology of the samples was studied by scanning electronic microscopy (Quanta 200 SEM / FEG microscopes).

3. RESULTS AND DISCUSSION

3.1 Photocatalytic Activities

Because of a strong competition between water and VOC molecules for active sites over the TiO₂ surface, resulting in a considerable decrease in photocatalytic activity (Demeestere 2004), the test was carried out in dry air.

The contribution of adsorption phenomena in the process of toluene conversion on the sample surfaces was examined in dark conditions. The results show that Degussa P25, in spite of its relatively high specific surface area (~ 50 m²/g), manifests negligible adsorption capacities (C_{ads}) for toluene vapour. Concerning the adsorption capacities of porous composite samples having only 5 ÷ 7 times more developed specific surface area, their C_{ads} exceeds that of Degussa P25 by a factor of 10² (Tab. 2, Samples 1, 2 and 5).

Table 2. Photocatalytic activities of samples in the total toluene oxidation reaction

| N° | Sample | Fabrication method | C _{ads} in dark (mg/gcat) | A _{photocat} (µg/mgTiO ₂ * h) | TiO ₂ content (mg) |
|----|---|----------------------------------|------------------------------------|---|-------------------------------|
| 1 | SiO ₂ – TiO ₂ -a | CVD-MLM1 | 1.40 | 4.10 | 60 |
| 2 | γAl ₂ O ₃ – TiO ₂ -a | CVD-MLM1 | 0.90 | 1.80 | 60 |
| 3 | SiO ₂ – TiO ₂ -c | CVD-MLM2 | - | 5.50 | 45 |
| 4 | γAl ₂ O ₃ – TiO ₂ -c | CVD-MLM2 | - | 4.15 | 30 |
| 5 | Degussa P25 | Physical adhesion over cardboard | 0.01 | 0.35 | 60 |

Under UV irradiation (Fig. 2), the photocatalytic activity of the Degussa P25 sample completely ceased within 3 hours. The photocatalytic activities of the silica- and alumina-based composites containing amorphous TiO₂ aggregates ceased after much longer periods of time (45 and 20 hours, respectively).

The amorphous and crystalline silica-based composites manifest the highest photocatalytic activities (Fig. 2 and Tab. 2). Besides a particular role of an oxide support in the promotion of the photocatalytic capacities of composite structures [Evstratov et al. (2005)], this phenomenon could be probably caused by an exceptional adsorption capacity of the silica-based composites (Fig. 2) with the most developed specific surfaces.

For VOC molecules being strong Lewis bases, the most attractive adsorption active sites are the Lewis acceptor centers, and the most powerful ones, among all the tested samples, occur over the surfaces of the silica-based composites (Si⁴⁺) [Noller et al. 1981]. Strong donor-acceptor interactions in these pre-adsorbed systems reduce their chemical stability and so favor their rapid degradation by powerful secondary active forms O²⁻ and OH[°] during the final process stage.

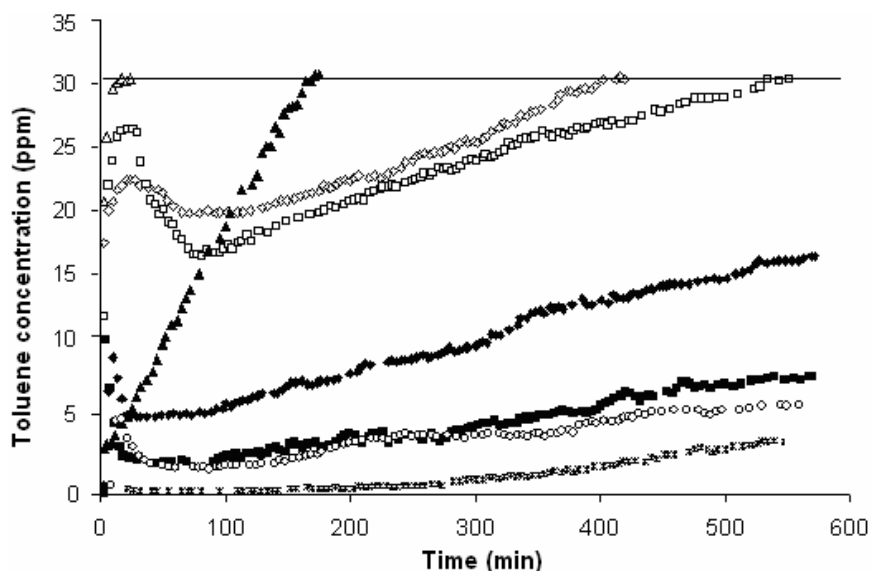


Fig. 2. Evolution of toluene outlet concentration over time ($\varphi = 0\%$):
 Δ – Deg. P25 dark; \square – SiO₂-TiO₂ (CVD-MLM1) dark; \diamond – γ Al₂O₃ -TiO₂ (CVD-MLM1) dark;
 \blacktriangle – Deg. P25 UV light; \blacksquare – SiO₂-TiO₂ (CVD-MLM1) UV light; \blacklozenge – γ Al₂O₃-TiO₂ (CVD-MLM1) UV light;
 \circ – γ Al₂O₃ -TiO₂ (CVD-MLM2) UV light;
 \times – SiO₂-TiO₂ (CVD-MLM2) UV light;

For the photocatalytic materials limited in their adsorption capacities (for example, Degussa P25, Fig. 2), the contribution of pre-adsorption pollutant activation to the intensity of further photocatalytic degradation is considerably lower. This factor could be decisive in certain limitations of the photocatalytic activities of the powder semiconductor. It is to be noted that alternating the nature of the support enables the activities of composite photocatalysts to be managed independently of the crystalline states of their active component. Thus, for instance, amorphous SiO₂ – TiO₂-a and γ Al₂O₃ – TiO₂-a samples (Tab. 2, Samples 1 and 2), both having 60 mg of titanium dioxide over their surfaces, manifest photocatalytic activities which differ by a factor approximately in 2.3. However, the crystalline state of the active component also seems to be a very important factor: a crystalline sample γ Al₂O₃ – TiO₂-c impoverished in titanium dioxide content (30 mg) is 2.3 times more active than its amorphous analogue γ Al₂O₃–TiO₂-a containing 60 mg of TiO₂ (Tab. 2, Samples 4 and 2).

3.2. XRD data and SEM results

The analytical results obtained using a high performance XRD technique show that both silica- and alumina-based composite structures produced by the CVD-MLM1 method are completely amorphous (Curves (4) and (5), Fig. 3). Concerning the samples with crystallized active components produced by the CVD-MLM2 method, their crystalline structures correspond to a mixture of two crystalline forms: 70-80 % of anatase and 30-20 % of rutile (Curves (2) and (3), Figure 5). This phase repartition is really close to that of Degussa P25, the reference product.

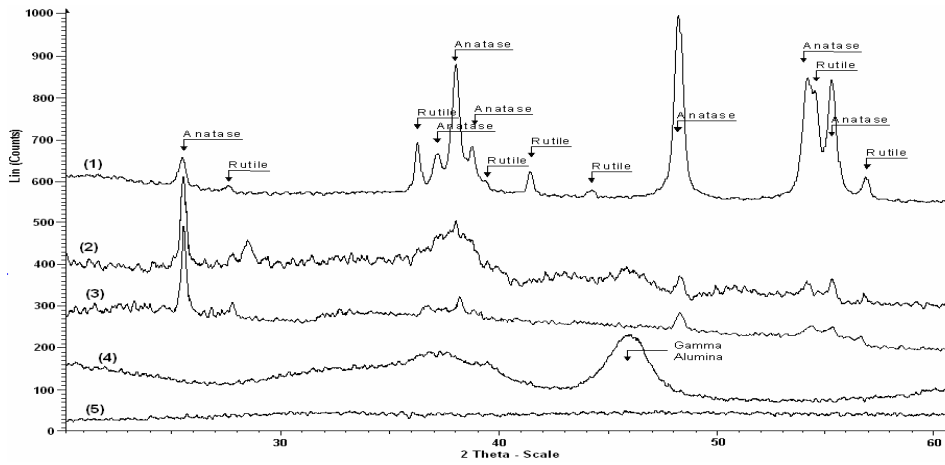


Fig. 3. Investigation of the sample crystalline state by XRD analysis:
 (1) Deg. P25; (2) $\gamma\text{Al}_2\text{O}_3$ - TiO_2 -c (CVD-MLM2); (3) SiO_2 - TiO_2 -c (CVD-MLM2);
 (4) $\gamma\text{Al}_2\text{O}_3$ - TiO_2 -a (CVD-MLM1); (5) SiO_2 - TiO_2 -a (CVD-MLM1)

SEM images (Fig. 4) demonstrate the appearance of new TiO_2 aggregates resulting from the CVD-MLM1 and CVD-MLM2 procedures.

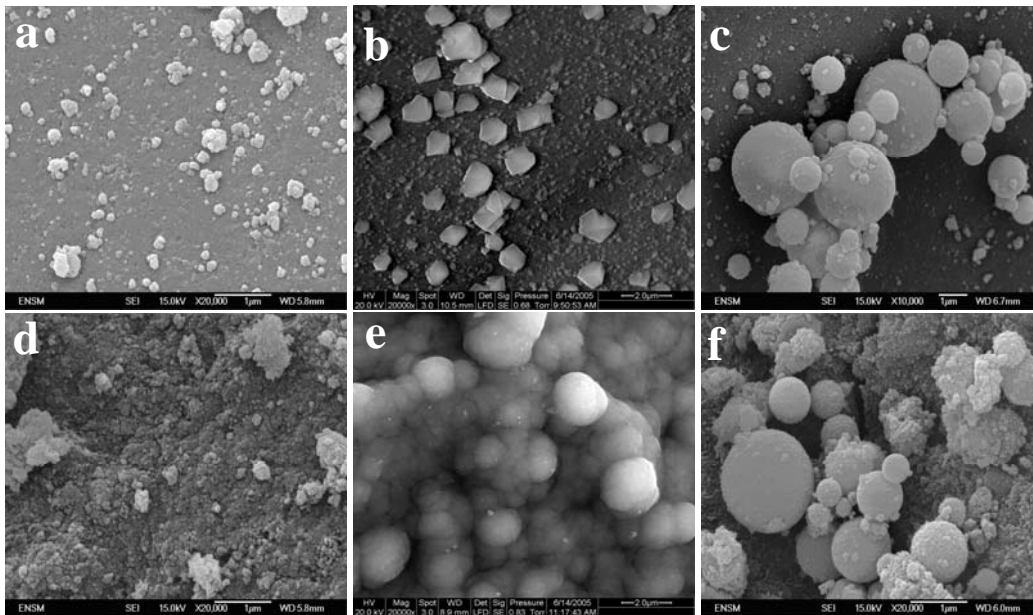


Fig. 4. SEM images of the surface structures:
 a). Pure SiO_2 ; b). SiO_2 + crystalline TiO_2 ; c). SiO_2 + amorphous TiO_2 ;
 d). Pure $\gamma\text{Al}_2\text{O}_3$; e). $\gamma\text{Al}_2\text{O}_3$ + crystalline TiO_2 ; f). $\gamma\text{Al}_2\text{O}_3$ + amorphous TiO_2

For silica-based crystalline samples, the active component aggregate sizes do not exceed 500 nm, their polyhedral forms are well shaped (Photo (b), Fig. 4). As to alumina-based composites containing crystalline TiO_2 , no individual aggregate can be

found at their surfaces: the active phase is a thin molten nanometric film (Photo (e), Fig. 4). The active component aggregates in all amorphous composites have an ideal spherical form. Their diameters differ from 500 to 2000 nm for silica-based structures (Photo (c), Fig. 4) and from 200 to 1000 nm for alumina-based products (Photo (f), Fig. 4).

3.3. Sterilisation Activity of Samples

The results of a preliminary investigation of the photobiological activity of amorphous silica-based composite are given in Figure 5.



Fig. 5. Bacterial colony development in Petri dishes under different experimental conditions

Two Petri dishes were used as recipient for monitoring bacterial colony development in two parallel laboratory tests. It can be noted that in the dish sectors 1 and 9 containing pure silica supports exposed to sunlight, 21 and 6 bacterial colonies, respectively, mushroomed in 20 hours of incubation. In sectors 3 and 11 containing sunlight-exposed amorphous SiO₂-TiO₂ CVD-MLM1 samples, only one colony was found, compared with 21 + 6 = 27 colonies mushroomed over an inert surface.

No bacterial colony was developed in sectors 2 and 10 where the amorphous composite samples of the same type were exposed to UV-A irradiation. These results suggest an important sterilisation capacity of the amorphous titanium dioxide composites under both UV-A and sunlight irradiation.

4. CONCLUSION

In spite of their internal structure disorder, the oxide-based composites containing non-crystalline nano- and micro-aggregates of titanium dioxide possess important photocatalytic activities exceeding the ones of unsupported crystalline TiO₂. In the case of moderately concentrated VOC-air mixtures, the significant adsorption capacities of silica- and alumina-based nanosized TiO₂ composites favour an intense formation of adsorption complexes reinforce the photocatalytic properties of the composite. The amorphous tested composites manifest significant sterilization capacities, under both UV-A and sunlight irradiation. The particular photocatalytic

properties of oxide-supported nanosized non-crystalline titanium dioxide composites seem to be really promising for the probable appearing of a new generation of photocatalytic materials.

BIBLIOGRAPHY

Amine-Khodja A., Boulkamh A. & Richard C., 2005. *Phototransformation of metobromuron in the presence of TiO₂*. Applied Catalysis B: Environmental, 59(3-4), 147–154.

Chang J.T., Su C.W. & He J.L., 2006. *Photocatalytic TiO₂ film prepared using arc ion plating*. Surface & Coatings Technology 200, 3027– 3034.

Demeestere K., Visscher A., Dewulf J., Leeuwen M. V. & Langenhove H. V., 2004. *A new kinetic model for titanium dioxide mediated heterogeneous photocatalytic degradation of trichloroethylene in gas-phase*. Applied Catalysis B: Environmental 54, 261–274.

Evstratov A., Chis C., Gaudon P., Ducourant B. & Jouffrey P., 2005. *Structures composites en état amorphe en tant que photocatalyseurs d'une nouvelle génération*. Récents Progrès en Génie des Procédés 92, L-14, p. 1-8.

Kaliwoh N., Zhang J.Y. & Boyd I.W., 2000. *Titanium dioxide films prepared by photo-induced sol-gel processing using 172 nm excimer lamps*. Surface and Coatings Technology 125(1-3), 424 – 427.

Lecheng L., Chu H., Hu X. & Yue P., 1999. *Preparation of heterogeneous photocatalyst (TiO₂/Alumina) by metallo-organic chemical vapour deposition*. Ind. Eng. Chim. Res., 38, 3381– 3385.

Ma Y., Qiu J., Cao Y., Guan Z. & Yao J., 2001. *Photocatalytic activity of TiO₂ films grown on different substrates*. Chemosphere 44, 1087–1092.

Malygin A.A., 1999. *The molecular layering method as a basis of chemical nanotechnology*. In Book: Natural Microporous Materials in Environmental Technology. Kluwer Academic Publishers, P. 487–495.

Noller H. & Parera J.M., 1981. *Active sites in catalysis. An approach based on coordination chemistry*. Journal of Research Institute of Catalysis of Hokkaido University 29(2) 95–99.

Stamate M.D., 2000. *Dielectric properties of TiO₂ thin films deposited by a DC magnetron sputtering system*. Thin Solid Films 372(1-2), 246–249.

Wang Z.M., Fang Q., Zhang J.Y., Wu J.X., Di Y., Chen W., Chen M.L. & Boyd I.W., 2004. *Growth of titanium silicate thin films by photo-induced chemical vapor deposition*. Thin Solid Films, 453-454, 167–171.

Yumoto H., Matsudo S. & Akashi K., 2002. *Photocatalytic decomposition of NO₂ on TiO₂ films prepared by arc ion plating*. Vacuum 65(3), 509-514.

Zhao J. & Yang X., 2003. *Photocatalytic oxidation for indoor air purification: a literature review*. Build Environment, 38, 645–654.

ACKNOWLEDGEMENTS

The authors acknowledge Mme. C. Blachere-Lopez for the technical support in biological tests.

Received at 03. 09. 2007

Revised: 26 .09. 2007

Accepted for publication 06. 10. 2007